Discover Oncology

Research

miR-1246 enhances chemo-resistance of polyploid giant cancer cells in H1299 cells by targeting GSK3β/β-catenin

Lili Wang[1] · Zien Yang[1] · Sining Xing[1] · Song Zhao[1] · Mingyue Ouyang[1] · Huiying Yu[1]

Received: 23 December 2024 / Accepted: 19 May 2025
Published online: 24 May 2025

Abstract
Non-small cell lung cancer (NSCLC) is characterized by a high mortality rate. Chemotherapy has been observed to potentially increase the prevalence of polyploid giant cancer cells (PGCCs), which may play a role in the development of chemo-resistance in NSCLC. The dysregulated expression of miR-1246 has been implicated in the modulation of gene expression related to drug resistance. Therefore, the objective of this study is to examine the role of miRNA-1246 in PGCCs and to elucidate its regulatory mechanisms. H1299 cells were treated with 100 nM docetaxel (Doc) for 24 h, then allowed to recover for 3 days to form polyploid giant cancer cells (PGCCs). The miRNA profiles of these PGCCs were analyzed, focusing on miR-1246. Transfection with miR-1246 mimics or inhibitors was performed, and various assays were used to assess the effects of miR-1246 inn PGCCs. The study found miR-1246 levels were significantly higher in PGCCs than in the original cells, affecting chemo-resistance, apoptosis, migration, and epithelial-mesenchymal transition. These findings suggested that NSCLC H1299 cells may employ polyploidy formation as a survival mechanism in response to docetaxel-based treatment, mediated by the miR-1246/GSK3β/β-catenin axis, ultimately leading to enhanced chemo-resistance.

Keywords Non-small cell lung cancer · Polyploid giant cancer cells · miR-1246 · GSK3β · β-catenin · Chemo-resistance

1 Introduction

Lung cancer is the leading cause of cancer-related mortality in the world, and 80% of lung cancer cases are non-small cell lung cancer (NSCLC) cases. Despite improvements in the early diagnosis and therapy of NSCLC, the 5-year overall survival rate has remained low at only 16% [1]. Chemotherapy is the most common treatment for advanced-stage NSCLC patients. Recent research evidence showed that chemotherapy could significantly increase the proportion of polyploid giant cancer cells (PGCCs) in vivo [2]. PGCCs constituted a dangerous subpopulation of cancer cells and usually contained a single giant cell nucleus or multiple nuclei. It was long assumed that these PGCCs cannot survive and die due to 'mitotic catastrophe' after multipolar cell division [3]. However, some evidences suggested that although most PGCCs succumbed to cell death, a small percentage of them survived and produced viable progeny [4, 5]. Moreover, a number of studies have shown that PGCCs were an especially histological feature of human tumors and were particularly prominent in late stage and drug resistant cancers [6, 7]. Chemotherapy drugs like platinum compounds, which damage DNA, and taxanes,

Supplementary Information The online version contains supplementary material available at https://doi.org/10.1007/s12672-025-02756-0.

✉ Huiying Yu, hyingy@sina.com | [1]Laboratory of Basic Medicine, General Hospital of Northern Theatre Command, Shenyang 110016, Liaoning, China.

which stabilize microtubules, could create PGCCs [8]. Time-lapse tracking showed that ovarian cancer PGCCs mainly formed through endoreplication after low-dose olaparib exposure, and using atypical cell division methods to produce resistant daughter cells capable of mitosis [9]. Altogether, these data suggested that PGCCs may play an important role in NSCLC drug resistance.

MicroRNAs (miRNAs), a class of small non-coding RNAs, are important post-transcriptional regulators of gene expression and are indispensable for physiological and pathological processes. Previous studies have proved that aberrant expression of miRNAs could result in affecting the expression of drug resistance genes, including MDR1 and MRP1 [10]. A study revealed that miRNA-1246 via targeting AXIN2 and GSK3β inhibited MDR1 expression and induced apoptosis in chemotherapy resistant leukemia cells [11]. Another study indicated that miR-1246 could act as a promoter of lung tumor cells metastasis partly due to down-regulating GSK-3β while up-regulating β-catenin [12]. However, the role of miRNA in PGCCs chemotherapy resistance and the underlying mechanism has not yet been reported.

Tumorigenesis may occur when oncogene mutations, tumor suppressor mutations, or mutations in Wnt pathway components lead to abnormal activation or dysfunction of this pathway [13, 14]. It is well known that β-catenin is the core molecule of the classic Wnt pathway. As lung cancer progresses, the Wnt pathway plays an important role in its progression [15]. In NSCLC, Wnt ligands bind to FZD and LRP5/6 receptors, leading to LRP5/6 phosphorylation and recruitment of DVL and AXIN, which inhibit GSK3β. This prevents β-catenin degradation, allowing it to accumulate, move to the nucleus, and activate Wnt target genes by interacting with TCF/LEF [16]. Wnt/β-catenin signaling influences epithelial-mesenchymal transition (EMT) by activating SNAIL, SLUG, and TWIST, which regulate E-cadherin and N-cadherin expression [17]. The clinical analysis of patients with lung adenocarcinoma revealed that elevated nuclear expression of β-catenin is correlated with poor prognosis. β-catenin enhances the transcriptional expression of the downstream stem cell marker Nanog, thereby inhibiting cancer cell differentiation and promoting cell proliferation [16]. USP5 acted as a positive regulator of Wnt/β-catenin signaling in NSCLC. Targeting USP5 with the small molecule WP1130 leaded to the degradation of β-catenin and demonstrated significant inhibitory effects on lung cancer growth and metastasis [18]. Additionally, ethacrynic acid, a loop diuretic, suppressed EMT in A549 cells by blocking NDP-induced Wnt signaling [19]. These findings suggested that β-catenin may serve as a potential target for the treatment of NSCLC.

In this work, we aimed to probe whether miR-1246 modulates the malignant behaviors of NSCLC-PGCCs by regulate GSK3β/β-catenin axis and hope to find a potential strategy for increasing the chemotherapeutic sensitivity of NSCLC.

2 Materials and methods

2.1 Materials

DMEM/F12 medium (BasalMedia, Shanghai, China), fetal bovine serum (FBS, BI, Israel), docetaxel (Doc, Selleck, USA), miR-1246 mimics and inhibitor (KeyGEN BioTECH, Jiangsu, China), IM-12 (Selleck, USA), propidium iodide (PI, Sigma-Aldrich, USA), Apoptosis kit (BD, USA), cisplatin (Selleck, USA), CCK8 (Daeil Lab Service, Korea), Trizol reagent (Sigma-Aldrich, USA), Lipofectamine 2000 reagent (Invitrogen, USA), paraformaldehyde (Sigma-Aldrich, USA), Triton X-100 (Sigma-Aldrich, USA), TUNEL detection kit (TUNEL, Roche, Switzerland), anti-Bcl-2, anti-Bax, anti-cleaved caspase 3, anti-N-Cadherin, anti-Snail, anti-GSK3β, anti-β-catenin, anti-MRP1and anti-MDR1 (Cell Signaling Technology, USA), GAPDH (Sigma-Aldrich, USA),SuperSignal™ West Pico PLUS Luminol/Enhancer (Thermo, USA).

2.2 Cell culture, transfection and treatment schedule

Human NSCLC cell line H1299 was purchased from ATCC. Cells were cultured in DMEM/F12 medium supplemented with 10% FBS in a 37 °C, 5% CO_2 incubator. In some experiment, when the cell density reached about 60–70%, cells were treated with 100 nM Doc for 24 h, and then allowed to recover for 3 days in regular medium [20]. In other experiment, when the cell density reached about 50–60%, cells were transfected with 50 nM miR-1246 mimics or inhibitor for 24 h. After transfection, cells were treated with 100 nM Doc for 24 h and then allowed to recover for 3 days in regular medium. The cells collected at this time were used as PGCC. For long-term cultures, PGCCs were continued to be cultured in regular medium for 21 days to observe the production of progeny cells, without the use of drug therapy during the cultivation period. In the reversal experiments, 5 μM IM-12 was added into the medium for 24 h before transfection.

2.3 Tissue samples

The paraffin-embedded NSCLC tissue samples (n = 11) were obtained from the Department of Pathology in General Hospital of Northern Theatre Command. All patients were histologically diagnosed of NSCLC (adenocarcinoma or squamous cell carcinoma) without any other cancer. All patients received paclitaxel (albumin bound) combined with cisplatin for 3 cycles. This study was approved by the Hospital Review Board and the confidentiality of patient information was maintained.

2.4 PGCC identification and counting

PGCCs exhibited heterogeneous distribution within tumor tissue sections, with frequent observation of hot spot fields. For this study, five hot spot fields were selected for evaluation at 400 × magnification. The nuclear size of PGCCs was measured using a micrometer on hematoxylin and eosin (HE)-stained tissue sections, following the criteria established in the previous research [21], which defined a PGCC as a tumor cell possessing a nucleus at least three times larger than that of a diploid tumor cell.

2.5 DNA content and cell cycle assay

5×10^5 cells were fixed in 80% iced methanol at −20 °C overnight, washed with PBS, centrifuged (1000 g × 5 min), and then stained with 50 μg/ml PI for 30 min in dark room. DNA content and cell cycle were analyzed by using a FACS CantoII flow cytometer (BD Biosciences).

2.6 Apoptosis analysis

A total of 5×10^5 cells were collected and washed twice with cold PBS, then resuspended in 500 μl of binding buffer containing 5 μl Annexin V-FITC and 5 μl PI for 15 min in the dark. Stained cells were subjected to flow cytometric analysis on a FACSCalibur instrument within 1 h, and a total of 10 000 events were acquired and analyzed using CellQuest software.

2.7 Drug-resistance assay

Cells were cultured in 96-well cell culture dishes, containing about 1×10^4 cells per well, and were cultured overnight at 5% CO_2 and 37 °C. Afterward, cells were incubated with various doses of Doc (1, 2, 4, 8, 16, and 32 μM, respectively) or cisplatin (1, 2, 4, 8, 16, and 32 μM, respectively) and were cultured for another 48 h. After 48 h incubation, cells were incubated with 10 μl CCK8 for an additional 4 h at 37 °C in an atmosphere of 5% CO_2. The absorbance was measured at 450 nm using a microplate reader (Thermo, USA). The results were represented as inhibition rate (%), as described previously [22]. The growth inhibition rate was calculated using the following formula: the inhibition rate = (absorbance of experimental group—absorbance of control group) / (absorbance of experimental group—absorbance of blank group) × 100%.

2.8 Live/dead staining assay

Cells were plated in a 96-well clear bottom plate (5000 cells per well; Corning, NY, USA, #3610) overnight and supplemented with regular medium. Incucyte Cytotox Green Dye (Sartorius, Gottingham, Germany, #4633) diluted in complete medium (5 μM final concentration) was added to each well. Cell live/dead staining was assessed using Incucyte® Live Cell Imaging (IncuCyte® Live-Cell Analysis System S3). Cells were imaged in phase contrast and green fluorescence every 6 h for a total of 48 h.

2.9 miRNA sequence analysis

The miRNA profiles in PGCCs and the control cells were sequenced by Illumina HiSeq™ 2500 after the samples were sent to Hoogen Biotech Shanghai Company (Shanghai, China). The raw reads were processed using miRDeep2. Normalization and differential expression analysis were executed using DESeq2 with the default configuration. The fold changes in the expression of individual miRNA were calculated. The differentially expressed miRNAs (DEmiRNAs) with

$|\log_2 FoldChange| > 1$ and $P < 0.05$ were considered to be significant. Then, the heatmap was generated using the ggplot2 package in the R software.

2.10 miRNA target prediction analysis

Gene targets of miR-1246 were predicted using four miRNA target prediction databases: miRBD, miRWalk, TargetScan and miRTarBase. Only genes predicted by four databases together could be selected, taking intersection.

2.11 Dual luciferase reporter assay

Using the 3′-UTR of the GSK3β fragment, the wild-type (WT) or mutant (MUT) binding sites for miR-1246 were cloned into the pmirGLO luciferase reporter vector (KeyGen Biotech, China). In 96-well plates, 2×10^4 cells were transfected with miR-1246 mimics/negative control of mimics, as well as reporter plasmids (pmirGLO-GSK3β-WT and pmirGLO-GSK3β-MUT) using Lipofectamine 2000 reagent (Invitrogen, USA). Following transfection, the activity of luciferase was measured 48 h later.

2.12 Real-time quantitative polymerase chain reaction (RT-qPCR)

The total RNA of cells was extracted using the Trizol reagent according to the manufacturer's instructions. Analyzing the absorbance at 260 nm and 280 nm allowed us to determine the concentration and purity of the RNA. RT-qPCR was performed on a real-time PCR system using SYBR-Green I (ABI 7500, Takara, Japan). The reaction procedure was as follows: 95 °C for 3 min, 95 °C for 30 s, 58 °C for 30 s by 40 cycles. The expression of miR-1246 was calculated normalized to U6 with $2^{-\Delta\Delta Ct}$ method.

2.13 Immunofluorescence staining

1×10^5 cells were washed with PBS and fixed with 4% paraformaldehyde. Following PBS washing, cells were permeabilized with 0.3% Triton X-100 in PBS for 10 min, and blocked for 1 h in 5% BSA. Anti-cleaved caspase 3 antibody (1:250, cell signaling, #9664) or anti-Ki67 antibody (1:200, abcam, ab16667) was incubated with cells overnight at 4 °C. Incubation with goat anti-rabbit secondary antibody (1:1 000) for 2 h occurred the next day. Cells were counterstained with DAPI (1:100) and phalloidin (1:200) to visualize the nucleus and photographed by a fluorescent microscope (Nikon, Japan).

2.14 TdT-mediated dUTP nick-end labeling (TUNEL) analysis

Assays for TUNEL were carried out using the TUNEL detection kit as instructed. Briefly, cells were fixed in 4% paraformaldehyde at room temperature for 30 min. For permeabilization of the cells, 0.3% Triton X-100 was added in PBS after PBS washing. Subsequently, 50 µl the TUNEL reaction mixture was added and incubated in a dark, humidified environment for 1 h at 37 °C. The cells were stained with DAPI and visualized with a fluorescent microscope.

2.15 Wound-healing assay

1×10^6 cells were seeded in 60 mm cell culture dishes and grown to 90% confluence. The cellular monolayer was scratched with a 200 ml pipette tip to create a wound. Subsequently, the cells were further washed three times with PBS and images of the wound were taken under an inverted microscope (Nikon, Japan) at the indicated time-points (0 and 24 h).

2.16 Transwell migration assay

Cells were plated in the upper chamber at a density of 1×10^5 cells/ml in 100 µl serum free media, 500 µl culture media with 20% FBS was in the lower chamber. After incubation for 48 h, cells on the upper surface of the membrane were removed and migrant cells on the lower surface were fixed with 4% paraformaldehyde for 30 min and stained with crystal violet solution to each well for 10 min. Washed with PBS, and observed under an inverted microscope (Nikon, Japan) after drying. Five visual fields in the center and around were taken and counted.

2.17 Western blot

The total proteins were extracted by RIPA lysis buffer, separated via SDS-PAGE in 6–12% gels and transferred onto polyvinylidene difluoride membranes. The membranes were blocked with TBS-T containing 5% nonfat milk for 2 h followed by incubation in appropriate primary antibodies (anti-GSK3β (1:1000, cell signaling, #9315), anti-P-GSK3β(Ser9) (1:1000, cell signaling, #9323), anti-β-catenin (1:1000, cell signaling, #8480), anti-Bcl-2(1:2000, cell signaling, #2870), anti-Bax(1:2000, cell signaling, #2772), anti-Snail (1:1000, cell signaling, #3879), anti-N-Cadherin (1:1000, cell signaling, #13116), GAPDH (1:5000, sigma, G9545) and β-actin (1:3000, cell signaling, #3700)) overnight at 4 °C. Were purchased from Cell Signaling Technology (MA, USA). Next, the membranes were incubated with the indicated HRP-conjugated secondary antibodies for 2 h. SuperSignal™ West Pico PLUS Luminol/Enhancer was used for detection. Densitometric analysis was performed with Image J software. Relative expression level of target protein = the gray value of the target protein band / the gray value of the internal band (GAPDH).

2.18 Statistical analysis

All statistical comparisons were performed using GraphPad Prism 9.0 software. The data from three independent experiments were presented as the means ± standard deviation (SD). Using ANOVA analysis, followed by Holm-Sidak's multiple comparison tests or an unpaired t-test, the differences among/between groups were analyzed. The statistical significance was defined as $P < 0.05$.

3 Results

3.1 NSCLC cells survived as a form of PGCCs following docetaxel-based treatment

H1299 cells were treated with 100 nM Doc for 24 h, then removed drug and allowed to grow in normal culture medium for 3 days. The surviving cells entered an endoreplication cell cycle and grew as PGCCs. Based on Zhang et al.'s definition, PGCCs had nuclei that were at least three times larger than those of diploid cancer cells [23]. The cell volume of PGCCs was significantly increased, the nucleus was multinucleated and PGCCs were positive for Ki67 (Fig. 1A). As revealed by the analysis of DNA content using flow cytometry, the mean ploidy of the PGCCs group was (8.50 ± 0.10) N, significantly more than that in the control group (2.76 ± 0.20) N (Fig. 1B). Cell cycle analysis revealed that PGCCs exhibited cell cycle arrest at G_2/M phase (Fig. 1C). In the PGCCs group, the apoptosis rate was significantly lower than that in the control group (Fig. 1D). On the other hand, the PGCCs group is less sensitive to Doc and cisplatin compared to the control group (Fig. 1E, F). Next, we examined the existence of PGCCs in NSCLC tissue before and after chemotherapy. We observed morphologically that PGCCs with giant or multiple nuclei were significantly present in human NSCLC tissue after chemotherapy, but PGCCs were basically not observed in human NSCLC tissue before chemotherapy (Fig. 1G). Taken together, the surviving cells after 3 days of Doc treatment were PGCCs, and these cells had stronger chemo-resistance ability than parental cells.

3.2 miR-1246 was involved in regulating PGCC chemo-resistance and the generation of progeny cells

To identify the candidate miRNAs related to chemoresistance of PGCCs, we performed miRNA sequencing. The results revealed that 49 miRNAs were upregulated, and 42 miRNAs were downregulated in the PGCCs group compared with the control group (Supplementary Table S1). The top 10 up-regulated and down-regulated DEmiRNAs between PGCCs and control were shown in Fig. 2A. Among the top 10 up-regulated miRNAs, we further confirmed a significant up-regulation of miR-1246 in PGCCs by RT-qPCR (Fig. 2B).

To manipulate the cellular levels of miR-1246, its mimics and inhibitor were transfected into H1299 cells. RT-qPCR analysis indicated that miR-1246 was up-regulated compared to negative control of mimics (NC), and was down-regulated compared to negative control of inhibitor (NC) in PGCCs (Fig. 2C, D). To testify whether the level of miR-1246 was related with chemotherapy resistance of PGCCs, CCK-8 assay was performed to measure cytotoxicity of Doc or cisplatin after transfection of miR-1246 mimics or inhibitor. The results showed that up-regulation of miR-1246 significantly increased Doc or cisplatin resistance of PGCCs (Fig. 2E, F), whereas down-regulation of miR-1246 decreased

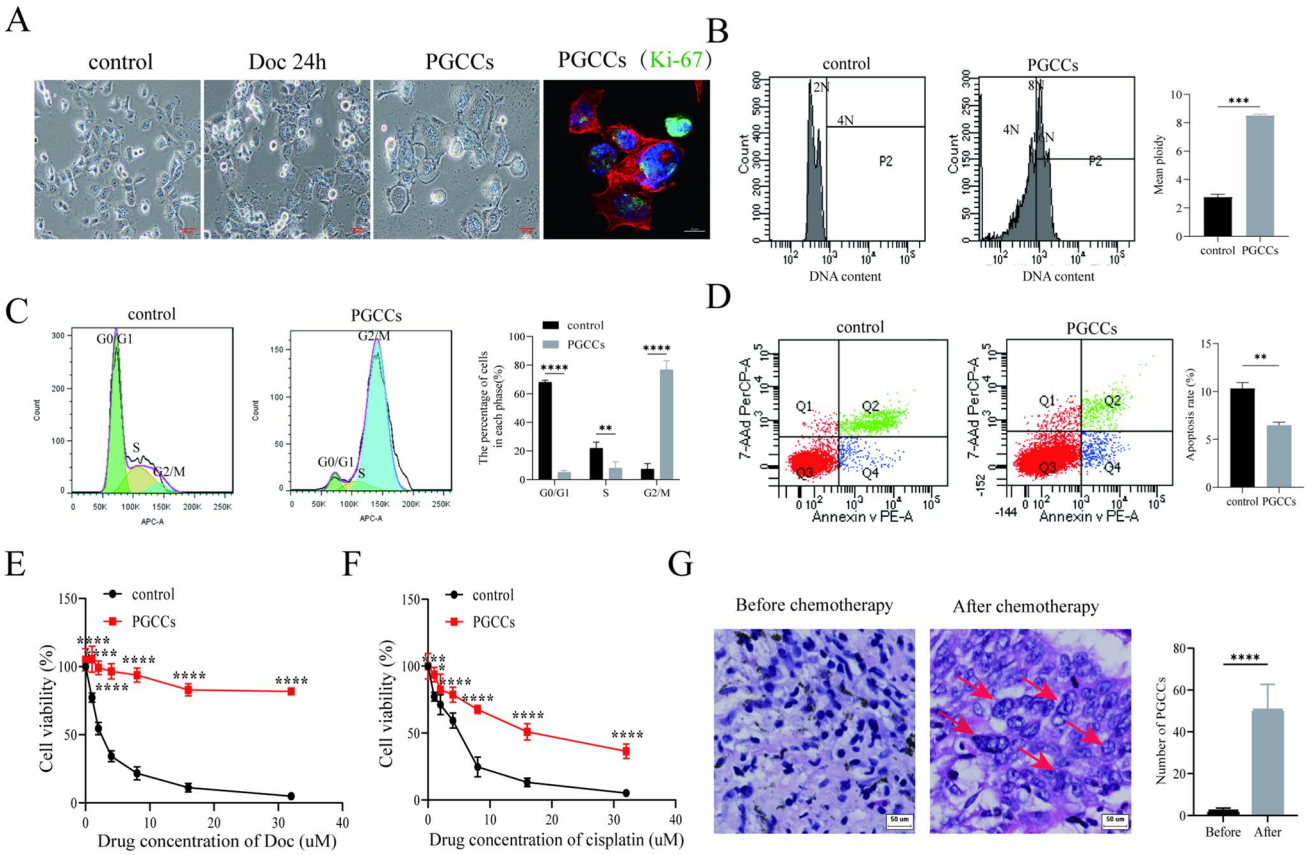

Fig. 1 PGCCs grew after docetaxel treatment. **A** Morphologic change of PGCCs after treating with 100 nM Doc for 24 h and then cultured in a drug-free medium for 3 days (×200), and PGCCs were stained with Ki-67antibody (Green: Ki-67-positive cells; Blue: DAPI; Red: phalloidin). **B** DNA content of PGCCs was analyzed by flow cytometry. **C** The cell cycle of PGCCs was detected by flow cytometry. **D** Apoptosis analysis of PGCCs was examined by flow cytometry. **E**, **F** The inhibition rates of PGCCs treated with Doc or cisplatin for 48 h were analyzed by CCK8 assay. **G** H&E staining of human NSCLC tissues (n = 11) were performed before and after 3 cycles of chemotherapy, and PGCCs were indicated by the red arrow. *****P < 0.0001*, ****P < 0.001*, ***P < 0.01*, **P < 0.05*

Doc or cisplatin resistance of PGCCs (Fig. 2G, H). As shown in Fig. 2I, compared with the NC group, the mRNA levels of MRP1 and MDR1 were decreased significantly in miR-1246 inhibitor-transfected PGCCs, while the mRNA levels of MRP1 and MDR1 were increased significantly in PGCCs transfected by miR-1246 mimics. After 7 days of recovery, PGCCs remained dormant, and the cell size continued to increase in both the miR-1246 inhibitor group and the NC group. For the next 7 days, some small daughter cells began to bud from PGCCs in the NC group. As the time spent in recovery culture increased, many smaller daughters' cells were generated via cell divisions in the NC group, but PGCCs remained dormant in the miR-1246 inhibitor group (Fig. 2J). The results suggested that down-regulation of miR-1246 could decrease the chemo-resistance and inhibit the generation of progeny cells of PGCCs.

3.3 Inhibition of miR-1246 induced apoptosis of PGCCs

Given that down-regulation of miR-1246 decreased chemo-resistance of PGCCs, the effect of miR-1246 on apoptosis was investigated. According to immunofluorescence staining, cleaved caspase 3 was elevated in miR-1246 inhibitor group but obviously reduced in miR-1246 mimics group compared with the NC group (Fig. 3A). Similarly, TUNEL fluorescence staining showed that the TUNEL positive signal was increased in miR-1246 inhibitor group compared with the NC group (Fig. 3B). Next, the mRNA and protein levels of anti-apoptotic molecular Bcl-2 were decreased while pro-apoptotic molecular Bax and cleaved caspase 3 were elevated with downregulated miR-1246 expression (Fig. 3C, D). The results showed that down-regulation of miR-1246 could induce apoptosis of PGCCs.

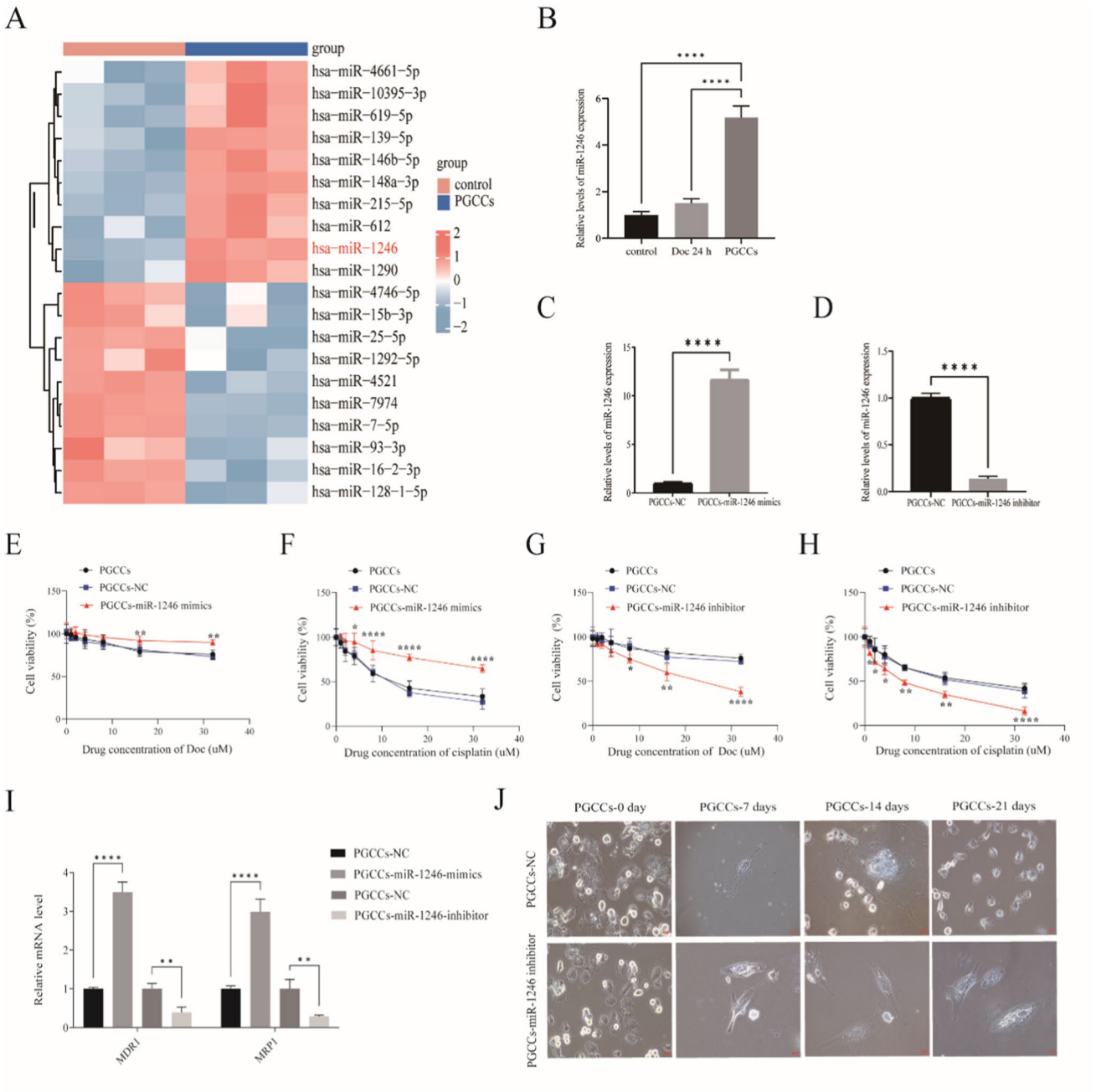

Fig. 2 Downregulation of miR-1246 decreased chemo-resistance and inhibited the generation of progeny cells of PGCCs. **A** Heatmap showing differential expression of top 20 miRNA (10 upregulated and 10 downregulated) between PGCCs and control cells. **B** The expression of miR-1246 in PGCCs was analyzed by RT-qPCR. **C**, **D** RT-qPCR analysis of miR-1246 expression in PGCCs on transfection with either miR-1246 mimics or miR-1246 inhibitor. **E**, **F** After transfection of miR-1246 mimics, PGCCs were treated with various concentrations of Doc or cisplatin for 48 h and then determined by CCK8 assays. **G**, **H** After transfection of miR-1246 inhibitor, PGCCs were treated with various concentrations of Doc or cisplatin for 48 h and then determined by CCK8 assays. **I** The mRNA expression levels of chemo-resistance relative molecule (MRP1 and MDR1) in PGCCs after transfected with miR-1246 mimics or miR-1246 inhibitor was determined by RT-PCR. **J** PGCCs generated small daughter cells over long-term cultivated for 21 days (200×). *****P < 0.0001*, ****P < 0.001*, ***P < 0.01*, **P < 0.05*

3.4 Inhibition of miR-1246 inhibited migration and the expression of EMT related markers of PGCCs

To evaluate the regulation of miR-1246 on PGCCs migration, wound healing assay was conducted, and the results showed overexpression of miR-1246 significantly enhanced the recovery from scratch-induced damage, whereas

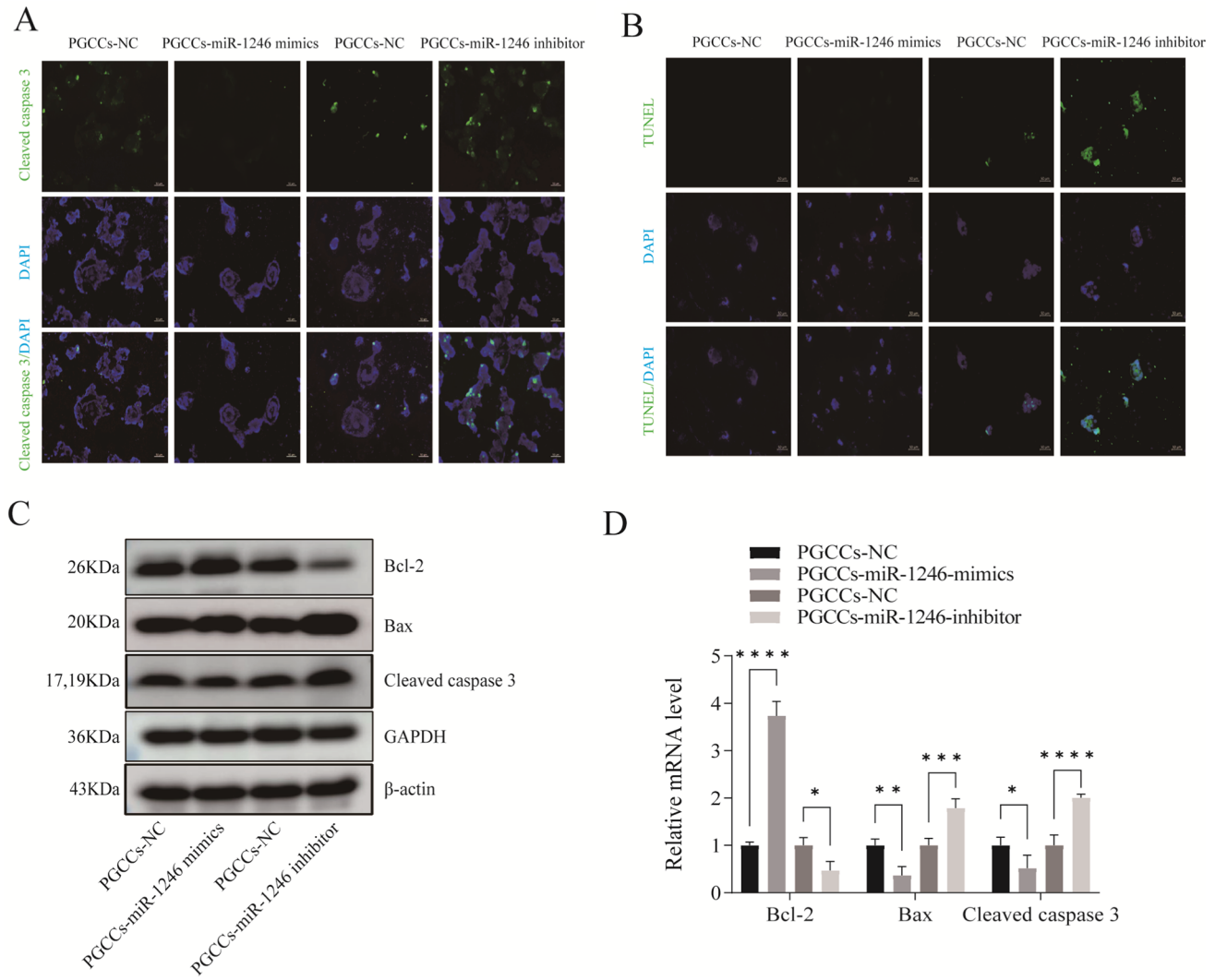

Fig. 3 Downregulation of miR-1246 induced apoptosis of PGCCs. **A** PGCCs were stained with Cleaved caspase 3 antibody after transfected with miR-1246 mimics or miR-1246 inhibitor (Green: Cleaved caspase 3-positive cells; Blue: DAPI). **B** PGCCs were stained with TUNEL dye after transfected with miR-1246 mimics or miR-1246 inhibitor (Green:TUNEL-positive cells; Blue: DAPI). **C** The protein expression levels of apoptosis relative protein (Bcl-2, Bax and Cleaved caspase 3) in PGCCs after transfected with miR-1246 mimics or miR-1246 inhibitor were determined by Western blot. **D** The mRNA expression levels of apoptosis relative molecule (Bcl-2, Bax and Cleaved caspase 3) in PGCCs after transfected with miR-1246 mimics or miR-1246 inhibitor was determined by RT-PCR. *****P < 0.0001*, ****P < 0.001*, ***P < 0.01*, **P < 0.05*

downregulation of miR-1246 significantly reduced the closure of scratch wounds of PGCCs (Fig. 4A). Transwell migration assay also showed that overexpression of miR-1246 significantly promoted PGCCs migration, while downregulation of miR-1246 inhibited cell migration (Fig. 4B). Furthermore, overexpression of miR-1246 increased the mRNA and protein levels of EMT related proteins N-cadherin and snail expression, while miR-1246 inhibition decreased N-cadherin and snail expression in PGCCs (Fig. 4C, D). The results showed that downregulation of miR-1246 could inhibit migration and the expression of EMT related markers of PGCCs.

3.5 miR-1246 enhanced the chemo-resistance of PGCCs through regulating the GSK3β/β-catenin pathway

Subsequently, we investigated the underlying molecular mechanism of miR-1246 in PGCCs. As shown in Fig. 5A, GSK3β was identified as a potential target for miR-1246 via four online prediction databases (miRBD, miRWalk, TargetScan and miRTarBase), which is a negative regulator of Wnt/β-catenin signaling pathway and locates in the upstream of β-catenin (Supplementary Table S2). Based on the dual luciferase reporter assay results, transfection of miR-1246 inhibited the activity of luciferase in transfected pmirGLO-GSK3β-WT cells, whereas pmirGLO-GSK3β-MUT cells revealed no change

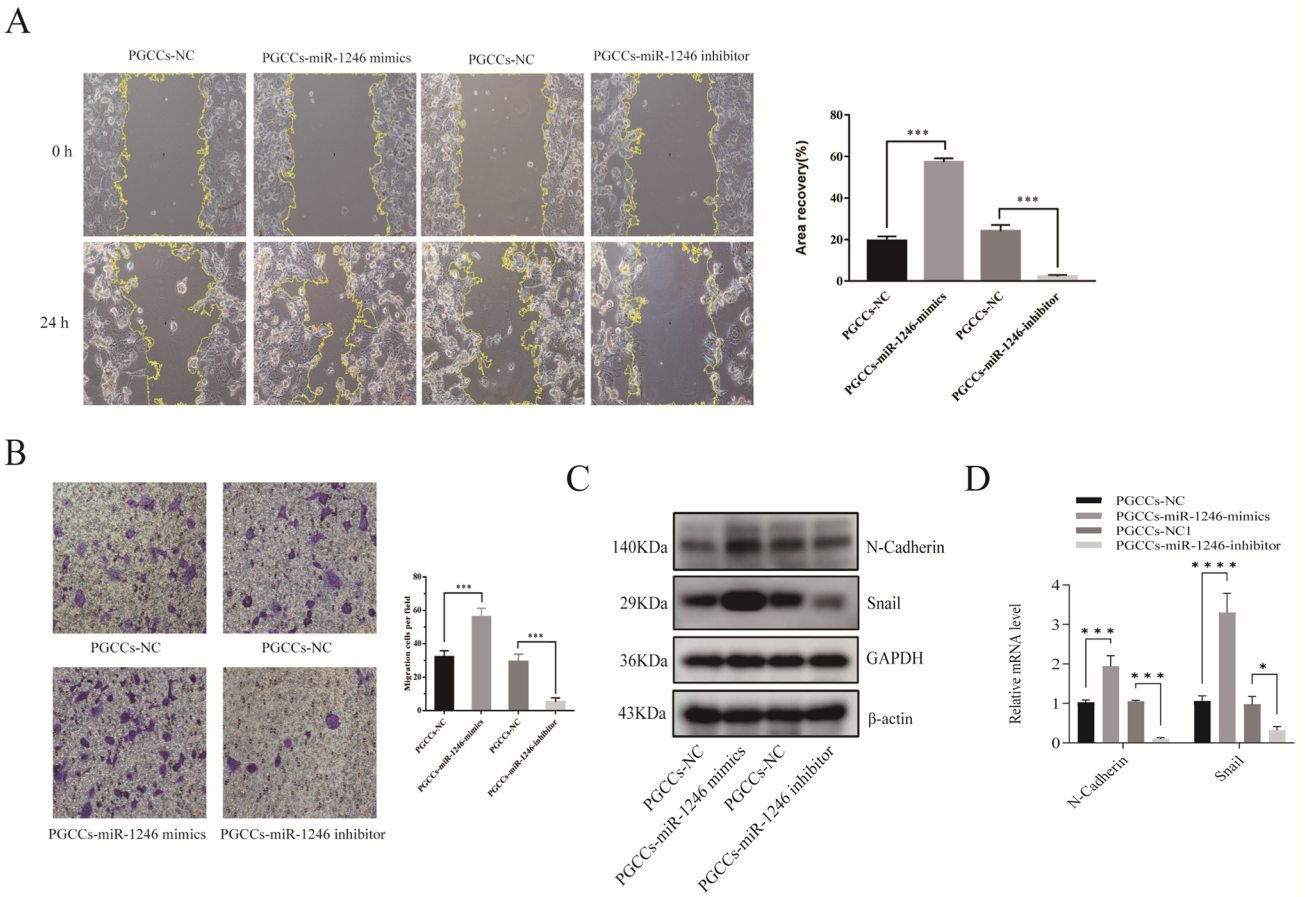

Fig. 4 Downregulation of miR-1246 inhibited migration and EMT of PGCCs. **A** Wound-healing assay evaluated the migration potential of PGCCs after transfected with miR-1246 mimics or miR-1246 inhibitor. **B** Transwell assay evaluated the migration potential of PGCCs after transfected with miR-1246 mimics or miR-1246 inhibitor. **C** The protein expression levels of EMT relative protein (N-cadherin and Snail) in PGCCs after transfected with miR-1246 mimics or miR-1246 inhibitor were determined by Western blot. **D** The mRNA expression levels of EMT relative relative molecule (N-cadherin and Snail) in PGCCs after transfected with miR-1246 mimics or miR-1246 inhibitor was determined by RT-PCR. *****P < 0.0001*, ****P < 0.001*, ***P < 0.01*, **P < 0.05*

in activity (Fig. 5B). Western blot and RT-PCR showed that overexpression of miR-1246 significantly decreased GSK3β expression, whereas downregulation of miR-1246 increased GSK3β expression (Fig. 5C, D). Then, IM-12 (a GSK3β inhibitor) was co-effected PGCCs with miR-1246 inhibitor. Wound-healing assay showed the migration ability was promoted in PGCCs-miR-1246 inhibitor + IM-12 group compared to PGCCs-miR-1246 inhibitor group (Fig. 5E). CCK8 assay and live/dead staining showed that compared with PGCCs-miR-1246 inhibitor group, the resistance of PGCCs-miR-1246 inhibitor + IM-12 group to docetaxel and cisplatin increased (Fig. 5F, G, H). Western blotting results showed that miR-1246 inhibitor partially reversed the expression of GSK3β, p-GSK3β and β-catenin induced by IM-12 (Fig. 5I). Meanwhile, miR-1246 inhibitor also partially reversed the expression of chemo-resistance relative gene (MRP1 and MDR1), apoptosis relative protein (Bcl-2 and Bax) and EMT relative protein (N-Cadhernin and snail) (Fig. 5I, J), which were all related to chemotherapy resistance of PGCCs. These results suggested that miR-1246/GSK3β/β-catenin axis may promote docetaxel resistance in NSCLC through increased survival of PGCCs.

4 Discussion

A long-term chemotherapy regimen will cause NSCLC patients to develop acquired resistance, which will lead to treatment failure and severe survival reductions [24]. Chemotherapy can cause PGCCs to form with a higher level of chromosome content than diploids [25]. Cancer is susceptible to genomic instability and chemo-resistance because of PGCCs, which are unique forms of plasticity [26]. In the past, cells with these abnormal morphologies were believed to be dying

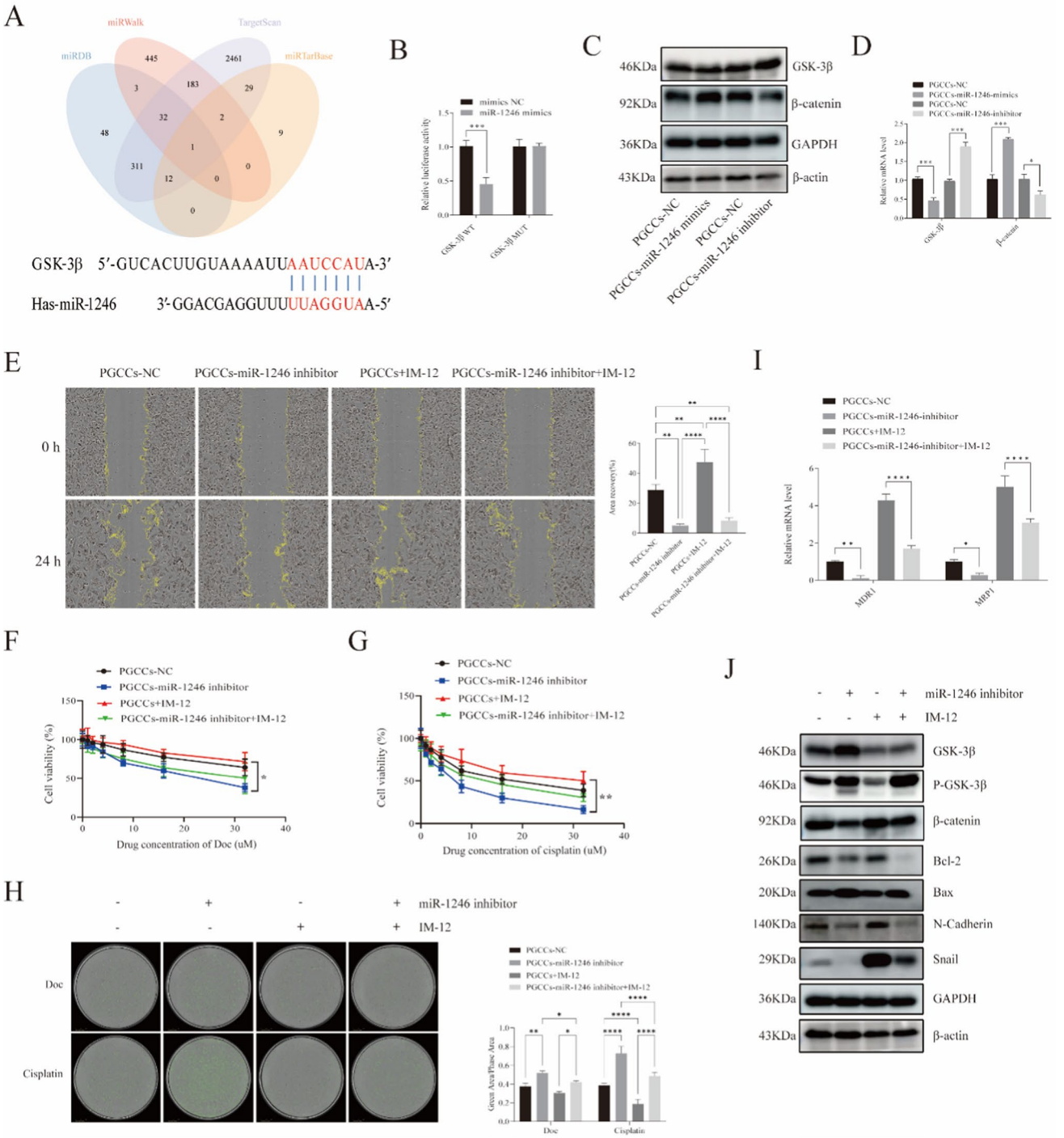

Fig. 5 miR-1246 enhanced the chemo-resistance of PGCCs through regulating the GSK3β/β-catenin pathway. **A** Potential binding sites between miR-1246 and GSK3β were predicted based on four miRNA target prediction databases (miRBD, miRWalk, TargetScan and miRTarBase). **B** Dual luciferase reporter assay the interaction of miR-1246 and GSK3β. **C** The influence of miR-1246 mimics or miR-1246 inhibitor on GSK3β and β-catenin expression in PGCCs was analyzed by western blot. **D** The mRNA expression levels of GSK3β and β-catenin in PGCCs after transfected with miR-1246 mimics or miR-1246 inhibitor was determined by RT-PCR. **E** Wound-healing assay evaluated the migration potential of PGCCs after transfected with miR-1246 inhibitor, then treated by IM-12. **F**, **G** After transfection of miR-1246 inhibitor or/and treated by IM-12, PGCCs were treated with various concentrations of Doc or cisplatin for 48 h and then determined by CCK8 assays. **H** The images of PGCCs were stained with a live/dead reagent on 48 h after transfected with miR-1246 inhibitor, then treated by IM-12. The dead cells were stained green. **I** The mRNA expression levels of chemo-resistance relative molecule (MRP1 and MDR1) in PGCCs after transfected with miR-1246 inhibitor or/and IM-12 was determined by RT-PCR. **J** miR-1246 inhibitor partially reversed the expression of related proteins in PGCCs was analyzed by Western blot. *****P < 0.0001*, ****P < 0.001*, ***P < 0.01*, **P < 0.05*

or irreversibly senescent, but now some PGCCs are being recognized as capable of overcoming this senescent cycle arrest and spawn progeny [27]. Furthermore, reversible polyploidization causes genome instability, which contributes to cancer development [28]. As a result of the PGCC life cycle, aneuploidy may develop as well as a myriad of copy number alterations [29]. By shuffling the genome, karyotype diversity becomes available for selection to act on during tumor evolution, especially during the development of drug resistance [30]. Recently, PGCCs have emerged as a promising field in cancer biology, and the ability of PGCCs to resist chemotherapy is still at the very beginning stages of our understanding.

This study reported that PGCCs was successfully induced and cultured from NSCLC cell line with Doc. Doc killed cancer cells by stabilizing microtubules and inhibiting mitosis, and may induce PGCCs through arresting cells in G_2-M phases [31]. Cell cycle arrest, special cell division types, and a higher genomic content are characteristics of NSCLC-PGCCs similar to those found in other cancers [23]. Moreover, we confirmed that Doc-induced PGCCs were anti-apoptosis and chemo-resistance. As evidence has grown that miRNAs play a role in chemo-resistance via multiple signaling pathways, miRNAs could be acting as oncogenes or tumor suppressors [32]. In the current study, we found that several miRNAs were differential expressed in PGCCs and their parental cells using miRNA sequence analysis. Among them, miR-1246 displayed obvious difference. Moreover, the overexpression of miR-1246 was most closely related to the drug resistance of cancer stem cell, and PGCCs had more similarities with cancer stem cell. Evidence has suggested that miR-1246 may influence proliferation, cell cycle progression, stemness and chemo-resistance of cancer cells to therapeutics [33]. Therefore, miR-1246 was selected for further validation among these DEmiRNAs.

The study investigated miR-1246's role in chemo-resistance in PGCCs. Findings revealed that reducing miR-1246 levels decreased chemo-resistance and lowered resistance-related molecules (MDR1 and MRP1), while increasing miR-1246 levels enhanced chemo-resistance. Emerging studies indicate that PGCCs could generate numerous small mononuclear cells through neosis, an asymmetric division aiding tumor repopulation [34]. This study found that PGCCs could form new cells, and miR-1246 downregulation inhibited this process, indicating a possible role of miR-1246 in PGCCs progeny formation. Additionally, miR-1246 downregulation was reported to inhibit tumor growth and promote apoptosis in laryngeal squamous cell carcinoma cells [35]. Our immunofluorescence staining, TUNEL assay and western blot demonstrated that reducing miR-1246 levels induced apoptosis in PGCCs by increasing pro-apoptotic Bax and decreasing anti-apoptotic Bcl-2. Conversely, miR-1246 overexpression inhibited apoptosis in these cells. Cancer cells gained chemotherapy resistance and transfer ability through trans-differentiation initiated by the EMT program, involving molecules such as N-Cadherin, E-Cadherin, Snail, and Vimentin [36, 37]. We suggest that reducing miR-1246 could inhibit PGCC migration and EMT by lowering N-cadherin and snail expression. We found miR-1246 is overexpressed in PGCCs, enhancing their chemo-resistance. Lowering miR-1246 could disrupt drug resistance by inhibiting EMT and inducing apoptosis.

To identify how miR-1246 affects chemo-resistance in PGCCs, bioinformatics tools predicted its targets, and GSK3β was confirmed as a target using a dual luciferase reporter assay. Our study found that miR-1246 could negatively regulate GSK3β expression, aligning with previous research. One study showed miR-1246 affected the Wnt/β-catenin pathway via GSK3β, promoting tumor metastasis in colorectal cancer [38]. A study found that miR-1246 promoted metastasis and invasion of A549 cells by targeting the GSK3β-mediated Wnt/β-Catenin pathway [12]. Another study found that miR-1246 inhibited the expression of GSK3β in lymphatic endothelial cells and promoted the expression of β-Catenin and its downstream MMP7, which in turn promoted lymphangiogenesis and lymphatic vessel remodeling [39]. However, there was currently no direct evidence linking miR-1246 to GSK3 β in PGCC chemotherapy resistance. GSK3β was crucial in the Wnt pathway, which significantly impacts tumor progression and drug resistance [40]. In this study, the results confirmed that repression of miR-1246 also decreased the expression levels of β-catenin. The miR-1246 inhibitor partially reversed the IM-12-induced expression of GSK3β, p-GSK3β and β-catenin, indicating a negative regulatory relationship between miR-1246 and GSK3β. Additionally, miR-1246 inhibitor could also partially reverse the expressions of MRP1, MDR1, Bcl-2, Bax, N-Cadhernin and snail induced by IM-12. Therefore, miR-1246 may affect the GSK3β/β-catenin pathway, contributing to drug resistance. In chemotherapy-resistant NSCLC patients with high miR-1246 expression, combining chemotherapy with miR-1246-targeted therapy could enhance treatment outcomes. However, miR-1246 might also target other genes, potentially causing unforeseen off-target effects.

In summary, miR-1246 may enhance chemo-resistance of PGCCs by regulating the GSK3β/β-catenin pathway in NSCLC. These findings may inform the development of a therapeutic model to ameliorate the resistance of NSCLC-PGCCs to chemotherapy. However, the limitation of this study was that it was only conducted on the H1299 cell line, which may not represent the full picture of NCSLC. In the future, we will verify this in more NCSLC cell lines. While the luciferase assay provides strong evidence of direct targeting, future studies involving rescue experiments would be valuable to fully establish causality. Meanwhile, further research will be conducted on the potential of combining miR-1246 inhibitors with existing chemotherapy drugs to enhance their efficacy in NSCLC.

Author contributions Huiying Yu and Lili Wang designed the experiments. Lili Wang, Zien Yang, Sining Xing, Song Zhao and Mingyue Ouyang performed the experiments. Lili Wang and Zien Yang analyzed the experiment data and wrote this manuscript. Huiying Yu reviewed the manuscript and supervised all the work. All authors approved the final version.

Funding The project was supported by grants from the Liaoning Provincial Natural Science Foundation Program (No. 2024-MS-250).

Data availability The datasets used and/or analyzed during the current study are available from the corresponding author upon reasonable request.

Declarations

Ethics approval and consent to participate This study was conducted in accordance with the Declaration of Helsinki and Good Clinical Practice guidelines. The study protocol was approved by the Institutional Review Board of the General Hospital of Northern Theatre Command (approval no.Y(2024)100). The requirement for informed consent was waived by the Institutional Review Board because of the study's retrospective nature.

Competing interests The authors declare no competing interests.

References

1. Siegel RL, Miller KD, Fuchs HE, Jemal A. Cancer statistics, 2021. CA Cancer J Clin. 2021;71(1):7–33.
2. Zheng M, Chen L, Fu J, Yang X, Chen S, Fu W, et al. Cdc42 regulates the expression of cytoskeleton and microtubule network proteins to promote invasion and metastasis of progeny cells derived from CoCl(2)-induced polyploid giant cancer cells. J Cancer. 2023;14(10):1920–34.
3. Mittal K, Donthamsetty S, Kaur R, Yang C, Gupta MV, Reid MD, et al. Multinucleated polyploidy drives resistance to Docetaxel chemotherapy in prostate cancer. Br J Cancer. 2017;116(9):1186–94.
4. Zhou X, Zhou M, Zheng M, Tian S, Yang X, Ning Y, et al. Polyploid giant cancer cells and cancer progression. Front Cell Dev Biol. 2022;10:1017588.
5. Liu P, Wang L, Yu H. Polyploid giant cancer cells: origin, possible pathways of formation, characteristics, and mechanisms of regulation. Front Cell Dev Biol. 2024;12:1410637.
6. Xuan B, Ghosh D, Dawson MR. Contributions of the distinct biophysical phenotype of polyploidal giant cancer cells to cancer progression. Semin Cancer Biol. 2022;81:64–72.
7. You B, Xia T, Gu M, Zhang Z, Zhang Q, Shen J, et al. AMPK-mTOR-mediated activation of autophagy promotes formation of dormant polyploid giant cancer cells. Cancer Res. 2022;82(5):846–58.
8. Alhaddad L, Chuprov-Netochin R, Pustovalova M, Osipov AN, Leonov S. Polyploid/multinucleated giant and slow-cycling cancer cell enrichment in response to X-ray irradiation of human glioblastoma multiforme cells differing in radioresistance and TP53/PTEN status. Int J Mol Sci. 2023;24(2):1228.
9. Zhang X, Yao J, Li X, Niu N, Liu Y, Hajek RA, et al. Targeting polyploid giant cancer cells potentiates a therapeutic response and overcomes resistance to PARP inhibitors in ovarian cancer. Sci Adv. 2023;9(29):eadf7195.
10. Chen Y, Li X, Shi L, Ma P, Wang W, Wu N, et al. Combination of 7-O-geranylquercetin and microRNA-451 enhances antitumor effect of Adriamycin by reserving P-gp-mediated drug resistance in breast cancer. Aging (Albany NY). 2022;14(17):7156–69.
11. Xie B, Li L, Zhang Z, Zhao L, Cheng J, Zhou C, et al. MicroRNA-1246 by targeting AXIN2 and GSK-3beta overcomes drug resistance and induces apoptosis in chemo-resistant leukemia cells. J Cancer. 2021;12(14):4196–208.
12. Yang F, Xiong H, Duan L, Li Q, Li X, Zhou Y. MiR-1246 promotes metastasis and invasion of A549 cells by targeting GSK-3β-mediated Wnt/β-catenin pathway. Cancer Res Treat. 2019;1(4):1420–9.
13. Hiremath IS, Goel A, Warrier S, Kumar AP, Sethi G, Garg M. The multidimensional role of the Wnt/beta-catenin signaling pathway in human malignancies. J Cell Physiol. 2022;237(1):199–238.
14. Doo DW, Meza-Perez S, Londono AI, Goldsberry WN, Katre AA, Boone JD, et al. Inhibition of the Wnt/beta-catenin pathway enhances antitumor immunity in ovarian cancer. Ther Adv Med Oncol. 2020;12:1758835920913798.
15. Chen J, Wang D, Chen H, Gu J, Jiang X, Han F, et al. TMEM196 inhibits lung cancer metastasis by regulating the Wnt/beta-catenin signaling pathway. J Cancer Res Clin Oncol. 2023;149(2):653–67.
16. Zhang Z, Westover D, Tang Z, Liu Y, Sun J, Sun Y, et al. Wnt/β-catenin signaling in the development and therapeutic resistance of non-small cell lung cancer. J Transl Med. 2024;22(1):565.

17. Li X, Lv F, Li F, Du M, Liang Y, Ju S, et al. LINC01089 inhibits tumorigenesis and epithelial-mesenchymal transition of non-small cell lung cancer via the miR-27a/SFRP1/Wnt/β-catenin axis. Front Oncol. 2020;10:532581.
18. Tung CH, Wu JE, Huang MF, Wang WL, Wu YY, Tsai YT, et al. Ubiquitin-specific peptidase 5 facilitates cancer stem cell-like properties in lung cancer by deubiquitinating β-catenin. Cancer Cell Int. 2023;23(1):207.
19. Zhang X, Huang C, Cui B, Pang Y, Liang R, Luo X. Ethacrynic acid enhances the antitumor effects of afatinib in EGFR/T790M-mutated NSCLC by inhibiting WNT/beta-catenin pathway activation. Dis Markers. 2021;2021:5530673.
20. Wang L, Ouyang M, Xing S, Zhao S, Liu S, Sun L, et al. Mesenchymal stem cells and their derived exosomes promote malignant phenotype of polyploid non-small-cell lung cancer cells through AMPK signaling pathway. Anal Cell Pathol (Amst). 2022;2022:8708202.
21. Lv H, Shi Y, Zhang L, Zhang D, Liu G, Yang Z, et al. Polyploid giant cancer cells with budding and the expression of cyclin E, S-phase kinase-associated protein 2, stathmin associated with the grading and metastasis in serous ovarian tumor. BMC Cancer. 2014;14:576.
22. Chen S, Yao L. Autophagy inhibitor potentiates the antitumor efficacy of apatinib in uterine sarcoma by stimulating PI3K/Akt/mTOR pathway. Cancer Chemother Pharmacol. 2021;88(2):323–34.
23. Zhang S, Mercado-Uribe I, Xing Z, Sun B, Kuang J, Liu J. Generation of cancer stem-like cells through the formation of polyploid giant cancer cells. Oncogene. 2014;33(1):116–28.
24. Wu J, Lin Z. Non-small cell lung cancer targeted therapy: drugs and mechanisms of drug resistance. Int J Mol Sci. 2022;23(23):15056.
25. Zhang K, Yang X, Zheng M, Ning Y, Zhang S. Acetylated-PPARgamma expression is regulated by different P53 genotypes associated with the adipogenic differentiation of polyploid giant cancer cells with daughter cells. Cancer Biol Med. 2023;20(1):56–76.
26. Jiao Y, Yu Y, Zheng M, Yan M, Wang J, Zhang Y, et al. Dormant cancer cells and polyploid giant cancer cells: the roots of cancer recurrence and metastasis. Clin Transl Med. 2024;14(2):e1567.
27. Saini G, Joshi S, Garlapati C, Li H, Kong J, Krishnamurthy J, et al. Polyploid giant cancer cell characterization: new frontiers in predicting response to chemotherapy in breast cancer. Semin Cancer Biol. 2022;81:220–31.
28. Adibi R, Moein S, Gheisari Y. Zoledronic acid targets chemo-resistant polyploid giant cancer cells. Sci Rep. 2023;13(1):419.
29. Erenpreisa J, Salmina K, Anatskaya O, Cragg MS. Paradoxes of cancer: survival at the brink. Semin Cancer Biol. 2022;81:119–31.
30. Heng J, Heng HH. Genome chaos: creating new genomic information essential for cancer macroevolution. Semin Cancer Biol. 2022;81:160–75.
31. Sharifi-Rad J, Quispe C, Patra JK, Singh YD, Panda MK, Das G, et al. Paclitaxel: application in modern oncology and nanomedicine-based cancer therapy. Oxid Med Cell Longev. 2021;2021:3687700.
32. Moghbeli M. MicroRNAs as the critical regulators of Cisplatin resistance in ovarian cancer cells. J Ovarian Res. 2021;14(1):127.
33. Dai YC, Pan Y, Quan MM, Chen Q, Pan Y, Ruan YY, et al. MicroRNA-1246 mediates drug resistance and metastasis in breast cancer by targeting NFE2L3. Front Oncol. 2021;11:677168.
34. Zhang Z, Feng X, Deng Z, Cheng J, Wang Y, Zhao M, et al. Irradiation-induced polyploid giant cancer cells are involved in tumor cell repopulation via neosis. Mol Oncol. 2021;15(8):2219–34.
35. Wu L, Zuo N, Pan S, Wang Y, Wang Q, Ma J. miR-1246 promotes laryngeal squamous cell carcinoma progression by interacting with THBS1. J Environ Pathol Toxicol Oncol. 2022;41(3):65–75.
36. Suresh Babu V, Bisht A, Mallipatna A, Sa D, Dudeja G, Kannan R, et al. Enhanced epithelial-to-mesenchymal transition and chemoresistance in advanced retinoblastoma tumors is driven by miR-181a. Cancers (Basel). 2022;14(20):5124.
37. Yuan D, Ma R, Sun T, Zhu K, Dang C, Ye H, et al. Knockdown of RSPH14 inhibits proliferation, migration, and invasion and promotes apoptosis of hepatocellular carcinoma via RelA. Cancer Cell Int. 2022;22(1):129.
38. Guo S, Chen J, Chen F, Zeng Q, Liu WL, Zhang G. Exosomes derived from Fusobacterium nucleatum-infected colorectal cancer cells facilitate tumour metastasis by selectively carrying miR-1246/92b-3p/27a-3p and CXCL16. Gut. 2022;71(2):e1–3.
39. Lu C, Xie L, Qiu S, Jiang T, Wang L, Chen Z, et al. Small extracellular vesicles derived from helicobacter pylori-infected gastric cancer cells induce lymphangiogenesis and lymphatic remodeling via transfer of miR-1246. Small. 2024;20(13):e2308688.
40. Zhang Y, Wang X. Targeting the Wnt/beta-catenin signaling pathway in cancer. J Hematol Oncol. 2020;13(1):165.